

# Mechanical behavior of composite beam aluminum-sandwich honeycomb strengthened by imperfect FGM plate under thermo-mechanical loading

Bensatallah Tayeb<sup>1,2</sup>, Rabahi Abderezak<sup>1,2</sup> and Tahar Hassaine Daouadji\*<sup>1,2</sup>

<sup>1</sup>Laboratory of Geomatics and Sustainable Development, University of Taret, Algeria

<sup>2</sup>Department of Civil Engineering, Ibn Khaldoun University of Taret, Algeria

(Received December 19, 2023, Revised February 2, 2024, Accepted February 9, 2024)

**Abstract.** In this paper, an improved theoretical interfacial stress analysis is presented for simply supported composite aluminum- sandwich honeycomb beam strengthened by imperfect FGM plate using linear elastic theory. The adherend shear deformations have been included in the present theoretical analyses by assuming a linear shear stress through the thickness of the adherends, while all existing solutions neglect this effect. Remarkable effect of shear deformations of adherends has been noted in the results. It is shown that both the sliding and the shear stress at the interface are influenced by the material and geometry parameters of the composite beam. This new solution is intended for application to composite beams made of all kinds of materials bonded with a thin plate. Finally, numerical comparisons between the existing solutions and the present new solution enable a clear appreciation of the effects of various parameters.

**Keywords:** adhesive bonding; aluminum-sandwich honeycomb composite beam; composite plate; interfacial stresses; shear lag effect; slip; strengthening

---

## 1. Introduction

An existing metal beam (for example steel or aluminum) can be retrofitted by bonding by composite materials plate to its soffit. This plate bonding technique has been used widely to retrofit steel beams, and has also been used to retrofit beams of other materials. The technique has numerous advantages such as increasing the strength and stiffness of an existing beam with minimal interference to the surrounding environment. Consequently, many studies have been carried out on the behavior and strength of such plated beams (Rabahi *et al.* 2023, Smith and Teng, 2002, Hassaine Daouadji *et al.* 2022, Benferhat *et al.* 2021, Hassaine Daouadji *et al.* 2020, Tounsi *et al.* 2008, Khadimallah 2020, Rabahi *et al.* 2021d, Mahmoud 2023, Yu-Hang 2020, Zine *et al.* 2020). In such retrofitted beams, debonding of the soffit plate from the beam is an important failure mode as it prevents the full ultimate flexural capacity of the retrofitted beam from being achieved. It is thus important to be able to predict the debonding failure load. Debonding failures

---

\*Corresponding author, Professor, E-mail: daouadjitahar@gmail.com, tahar.daouadji@univ-tiaret.dz

depend largely on the interfacial shear between the beam and the bonded plate. The determination of interfacial stresses has thus been researched for over the last few years for beams bonded with either steel or FRP plates. In particular, several relatively simple approximate closed-form solutions for interfacial stresses have been developed (AlFurjan 2021, Haytham *et al.* 2023a, Hassaine Daouadji 2017, Aman 2023, Benachour *et al.* 2008, Bentrar *et al.* 2023, Rabahi *et al.* 2022a, Rabahi *et al.* 2022b, Cuong-Le 2022, Khorasani *et al.* 2023, Katiyar 2022, Abdelhak *et al.* 2023, Bouakaz *et al.* 2014, BenHenni *et al.* 2021, Tlidji *et al.* 2022, Bensatallah *et al.* 2023, Benferhat *et al.* 2023, Kablia *et al.* 2023) based on a simple assumption for the adhesive layer as discussed later. Despite all of these studies, one striking fact is that the relationship between these existing solutions has not been established clearly in the existing literature (Benferhat *et al.* 2019, Hassaine Daouadji 2013, Rabahi *et al.* 2021b, Rabahi *et al.* 2021c).

With increasing demand and decreasing availability of resources in today's industrialized world, it is becoming increasingly necessary to explore opportunities for new sustainable building materials. The use of composite aluminum- sandwich honeycomb beam in civil engineering applications is limited due to its flexibility, shape, and the difficulties associated with establishing structural connections. Being an industrial product, composite aluminum- sandwich honeycomb exhibits variations of its mechanical properties more than other building materials, steel, concrete, or construction wood and may thus require a greater safety factor. Nonetheless, there are many researchers (Draiche *et al.* 2019, Hamrat *et al.* 2020, Rabahi *et al.* 2020, Rabahi *et al.* 2021a, Hassaine Daouadji *et al.* 2021, Haytham *et al.* 2023b, Addou *et al.* 2023, Alsubaie *et al.* 2023, Al-Osta *et al.* 2021, Belabed *et al.* 2024, Liu *et al.* 2022, Benferhat *et al.* 2018, Mesbah *et al.* 2023, Tounsi *et al.* 2023, Xia *et al.* 2023, Hassaine Daouadji *et al.* 2019, Van Vinh *et al.* 2022, Hakim *et al.* 2023, Kaddari *et al.* 2020) actively involved in overcoming these challenges, which confirms the potential of composite aluminum- sandwich honeycomb as a new structural material. Composite aluminum- sandwich honeycomb has excellent mechanical properties, including high tensile strength, toughness, and low weight, and has a shorter growth period with characteristics of large yield. Therefore, composite aluminum- sandwich honeycomb is considered a very suitable building material. Modern aluminum and sandwich honeycomb-based engineering materials can meet the current specifications of structural engineering, which enables large-scale applications of composite aluminum- sandwich honeycomb structures. Thus, there is a growing global interest and research in the use of sandwich honeycomb for various applications in engineering and construction. This work is focused on analytical and numerical solution on the static behavior of composite aluminum- sandwich honeycomb beam strengthened by imperfect FGM plate. Nowadays in many fields aluminum honeycomb structure is frequently used due to its stiffness to weight ratio, in-plane properties and low material and processing cost.

## **2. Theoretical analysis and solutions procedure**

### *2.1 Objective of this present research*

We have noticed that there are very few researchers in the world (according to the literature) who start the research axis on aluminum composite structures, and as there are industrial demands on the use of aluminum composite structures under thermo-mechanical loading. In this context and in order to meet the industrial need, we set the objective of treating the analytical analysis of the mechanical behavior of an aluminum-sandwich honeycomb composite beam reinforced by an

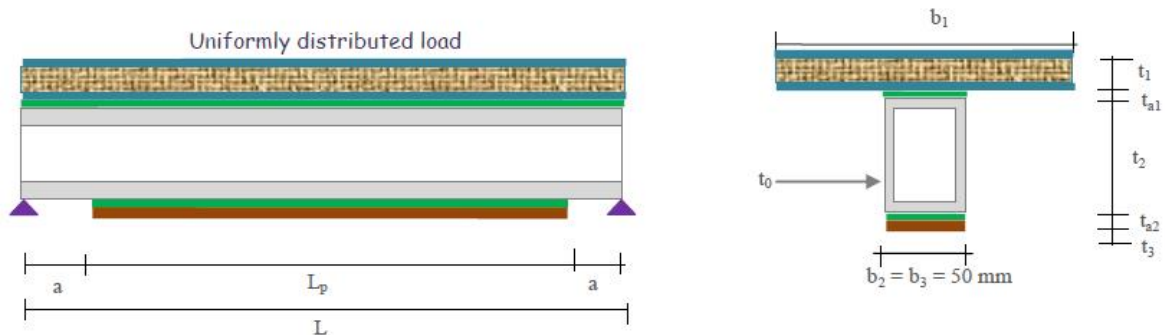


Fig. 1 Simply supported composite aluminum- sandwich honeycomb beam strengthened by imperfect FGM plate

imperfect FGM plate under thermo-mechanical loading. In this paper, it is shown that the stresses at the interface are influenced by the material and geometry parameters of the composite beam. I think this research is helpful for the understanding on mechanical behavior of the interface and design of the hybrid structures.

## 2.2 Assumptions and approaches

This analysis takes into account the transverse shear stress and deformation in the composite aluminum- sandwich honeycomb beam strengthened by imperfect FGM, but ignores the normal transverse stress. One of the analytical approaches for sandwich honeycomb slabs glued to the aluminum beam strengthened with imperfect FGM plate (Fig. 1) was presented in order to compare it with an analytical analysis from the literature (Hassaine Daouadji *et al.* 2021) for aluminum- sandwich honeycomb beam strengthened by imperfect FGM. All existing solutions are for linear elastic materials only. The key assumption in all of these solutions is that the adhesive layer is subject to shear stress that are constant across the thickness of the adhesive layer. It is this key assumption that enables relatively simple closed-form solutions to be obtained, although this assumption is somewhat hidden in some of the solutions.

The analytical approach is based on the following assumptions (Hassaine Daouadji *et al.* 2021):

- Elastic stress strain relationship for sandwich honeycomb slab, aluminum, hybrid imperfect FGM plate and adhesive;
- The composite aluminum beam is simply supported and shallow, i.e., plane sections remain plane in bending.
- There is an imperfect bond between the sandwich honeycomb slab and the aluminum beam; there will be a possibility of sliding between these two members.
- There is a perfect bond between the hybrid imperfect FGM plate and the aluminum beam; No slip is allowed at the interface of the bond hybrid imperfect FGM plate- aluminum beam (i.e., there is a perfect bond at the adhesive aluminum or imperfect FGM plate interface).
- The adhesive is supposed to play only one role in the transfer of stresses at a time: from the sandwich honeycomb slab to the aluminum beam, of the imperfect FGM plate and the aluminum beam.
- The stresses in the adhesive layer do not change through the direction of the thickness.
- The shear stress analysis assumes that the curvatures in the composite aluminum beam and

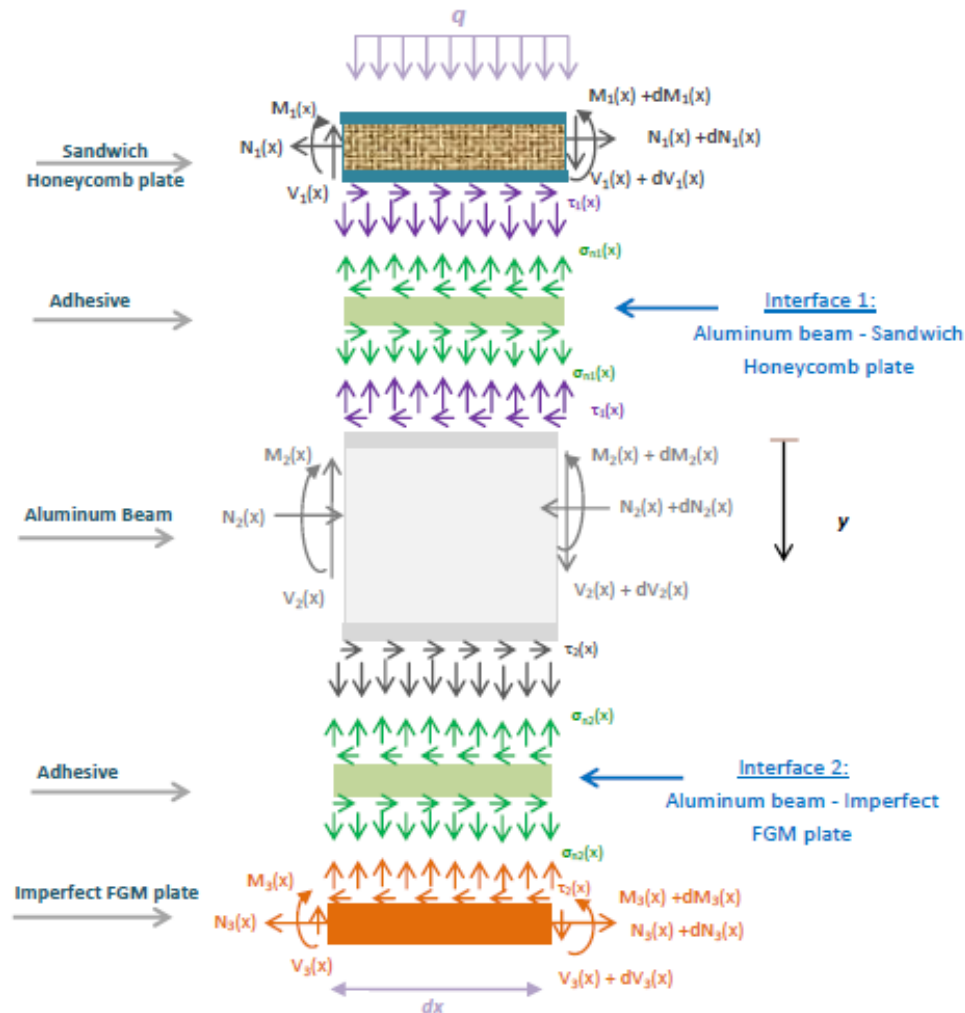


Fig. 2 Forces in infinitesimal element of a composite aluminum- sandwich honeycomb beam strengthened by imperfect FGM plate

imperfect FGM plate are equal (since this allows the shear stress and peel stress equations to be uncoupled). However, this assumption is not made in the normal stress solution, i.e., when the beam is loaded, vertical separation occurs between composite aluminum beam and imperfect FGM plate.

- A parabolic shear deformation distribution, through the depth of both the composite aluminum beam and the bonded imperfect FGM plate is assumed.
- Bending deformations of the composite aluminum beam and imperfect FGM plate are assumed.

A differential section  $dx$ , can be cut out from the composite aluminum- sandwich honeycomb beam strengthened by imperfect FGM plate, as shown in Fig. 2. The composite beam is made from four materials: imperfect FGM composite material, sandwich honeycomb, adhesive and aluminum beam. In the present analysis, linear elastic behavior is regarded to be for all the materials;

sandwich honeycomb, imperfect FGM composite material and aluminum beam, which must share in resisting the forces and moments caused by the transverse uniformly, distributed loads  $q$ . In the general case, the deformations that result must accommodate any interface slip in addition to the usual flexural and axial strains. Since sandwich honeycomb, composite laminate is an orthotropic material, its material properties vary from layer to layer. In analytical study (Hassaine Daouadji *et al.* 2021), the laminate theory is used to determine the stress and strain behaviors' of the externally bonded imperfect FGM plate in order to investigate the whole mechanical performance of the composite- strengthened structure.

The laminate theory is used to estimate the strain of the symmetrical sandwich honeycomb composite plate. In what follows, the stiffness of the reinforcement plate is significantly superior to that of the composite aluminum-sandwich honeycomb beam bonded by an imperfect FGM plate. The bending moment in the imperfect FGM plate can be neglected to simplify the shear stress derivation operations. On the other hand, the laminate theory is used to determine the stress of the externally bonded imperfect FGM plate in order to investigate the completely mechanical performance of the composite strengthened structure.

#### *Properties of the FGM constituent materials*

In this study, we consider an imperfect FGM plate with a volume fraction of porosity  $\delta$  ( $\delta \ll 1$ ), with different form of distribution between the metal and the ceramic. The modified mixture rule proposed by Benferhat *et al.* (2023) is

$$P = P_m(V_m - \frac{\delta}{2}) + P_c((\frac{z}{h} + \frac{1}{2})^k - \frac{\delta}{2}) \quad (1)$$

The modified mixture rule becomes

$$P = (P_c - P_m)(\frac{z}{h} + \frac{1}{2})^k + P_m - (P_c + P_m)\frac{\delta}{2} \quad (2)$$

Where,  $k$  is the power law index that takes values greater than or equals to zero. The FGM plate becomes a fully ceramic plate when  $k$  is set to zero and fully metal for large value of  $k$ . The Young's modulus ( $E$ ) of the imperfect FG plate can be written as a function of thickness coordinate,  $z$  (middle surface). The material properties of a perfect FGM plate can be obtained when the volume fraction of porosity  $\alpha$  is set to zero. Due to the small variations of the Poisson ratio  $\nu$ , it is assumed constant. Several forms of porosity have been studied in the present work, such as uniform distribution "O", "X", "V" and Inverted "V" as follows (Kablia *et al.* 2023), including the deferent's distribution forms of porosity which come in the forms below

- Uniform distribution shape of the porosity

$$E_2(z) = (e_c - e_m)((\frac{z}{t_2} + 0.5))^k + e_m - (e_c + e_m)\frac{\delta}{2} \quad (3)$$

- Form "X" distribution shape of the porosity

$$E_2(z) = (e_c - e_m)((\frac{z}{t_2} + 0.5))^k + e_m - (e_c + e_m)\frac{\delta}{2}(2\frac{z}{t_2}) \quad (4)$$

- Form "O" distribution shape of the porosity

$$E_2(z) = (e_c - e_m)((\frac{z}{t_2} + 0.5))^k + e_m - (e_c + e_m)\frac{\delta}{2}(1 - 2\frac{|z|}{t_2}) \quad (5)$$

- Form "V" distribution shape of the porosity

$$E_2(z) = (e_c - e_m)\left(\left(\frac{z}{t_2} + 0.5\right)\right)^k + e_m - (e_c + e_m)\frac{\delta}{2}\left(\frac{1}{2} + \frac{z}{t_2}\right) \quad (6)$$

- Inverted Form “V” distribution shape of the porosity

$$E_2(z) = (e_c - e_m)\left(\left(\frac{z}{t_2} + 0.5\right)\right)^k + e_m - (e_c + e_m)\frac{\delta}{2}\left(\frac{1}{2} - \frac{z}{t_2}\right) \quad (7)$$

Being given that  $E_2(z)$  is determined according to the form of distribution of the porosity in the imperfect FGM plate, given by the Eqs. (3), (4), (5), (6) and (7), the linear constitutive relations of a FGM plate can be written as

$$\begin{Bmatrix} \sigma_x \\ \sigma_y \\ \tau_{yz} \\ \tau_{xz} \\ \tau_{xy} \end{Bmatrix} = \begin{bmatrix} \frac{E_2(z)}{1-\nu^2} & \frac{\nu E_2(z)}{1-\nu^2} & 0 & 0 & 0 \\ \frac{\nu E_2(z)}{1-\nu^2} & \frac{E_2(z)}{1-\nu^2} & 0 & 0 & 0 \\ 0 & 0 & \frac{E_2(z)}{2(1+\nu)} & 0 & 0 \\ 0 & 0 & 0 & \frac{E_2(z)}{2(1+\nu)} & 0 \\ 0 & 0 & 0 & 0 & \frac{E_2(z)}{2(1+\nu)} \end{bmatrix} \begin{Bmatrix} \varepsilon_x \\ \varepsilon_y \\ \gamma_{yz} \\ \gamma_{xz} \\ \gamma_{xy} \end{Bmatrix} \quad (8)$$

Where  $(\sigma_x, \sigma_y, \tau_{xy}, \tau_{yz}, \tau_{yx})$  and  $(\varepsilon_x, \varepsilon_y, \gamma_{xy}, \gamma_{yz}, \gamma_{yx})$  are the stress and strain components, respectively, and  $A_{ij}, D_{ij}$  are the plate stiffness, defined by

$$A_{ij} = \int_{-h/2}^{h/2} Q_{ij} dz \quad D_{ij} = \int_{-h/2}^{h/2} Q_{ij} z^2 dz \quad (9)$$

Where  $A'_{ij}, D'_{ij}$  are defined

$$A'_{11} = \frac{A_{22}}{A_{11}A_{22} - A_{12}^2} \quad D'_{11} = \frac{D_{22}}{D_{11}D_{22} - D_{12}^2} \quad (10)$$

## 2.3 Stress analysis at interface 1: Aluminum beam- sandwich honeycomb slab

### 2.3.1 Shear stress distribution along the Aluminum-sandwich honeycomb interface

The governing differential equation for the interfacial shear stress is expressed as (Bensatallah *et al.* 2020)

$$\frac{d^2 \tau(x)}{K_s \cdot dx^2} - k_1 b_2 \left[ \frac{(y_1 + y_2)(y_1 + y_2 + t_{a1})}{E_1 I_1 + E_2 I_2} + \frac{1}{E_1 A_1} + \frac{1}{E_2 A_2} (\alpha_2 - \alpha_1) \Delta T \right] \tau(x) + k_1 \frac{(y_1 + y_2)}{E_1 I_1 + E_2 I_2} \cdot V_T(x) = 0 \quad (11)$$

Where

$$k_1 = \left[ \frac{t_{a1}}{G_{a1}} + \frac{t_1}{4G_1} + \frac{5t_2}{12G_2} \right]^{-1} \quad (12)$$

For simplicity, the general solutions presented below are limited to loading which is either concentrated or uniformly distributed over part or the whole span of the composite aluminum beam, or both. For such loading,  $\frac{d^2 V_T(x)}{dx^2} = 0$ , and the general solution to Eq. (11) is given by simplified form

$$\tau(x) = \phi_1 e^{\lambda \cdot x} + \phi_2 e^{-\lambda \cdot x} + \frac{k_1}{\lambda^2} \left( \frac{1}{E_1 A_1} + \frac{1}{E_2 A_2} \right) \cdot V_T(x) \quad (13)$$

$$\tau(x) = \phi_1 e^{\lambda \cdot x} + \phi_2 e^{-\lambda \cdot x} + \eta \cdot V_T(x) \quad (14)$$

Where

$$\lambda^2 = \frac{b_2 \left[ \frac{(y_1+y_2)(y_1+y_2+t_{a1})}{E_1 I_1 + E_2 I_2} + \frac{1}{E_1 A_1} + \frac{1}{E_2 A_2} + (\alpha_2 - \alpha_1) \Delta T \right]}{\frac{t_{a1}}{G_{a1}} + \frac{t_1}{4G_1} + \frac{5t_2}{12G_2}} \quad (15)$$

And

$$\eta = \frac{\frac{1}{E_1 A_1} + \frac{1}{E_2 A_2}}{b_2 \left[ \frac{(y_1+y_2)(y_1+y_2+t_{a1})}{E_1 I_1 + E_2 I_2} + \frac{1}{E_1 A_1} + \frac{1}{E_2 A_2} + (\alpha_2 - \alpha_1) \Delta T \right]} \quad (16)$$

$$\tau(x) = \phi_1 e^{\lambda \cdot x} + \phi_2 e^{-\lambda \cdot x} + \frac{\frac{1}{E_1 A_1} + \frac{1}{E_2 A_2}}{b_2 \left[ \frac{(y_1+y_2)(y_1+y_2+t_{a1})}{E_1 I_1 + E_2 I_2} + \frac{1}{E_1 A_1} + \frac{1}{E_2 A_2} + (\alpha_2 - \alpha_1) \Delta T \right]} V_T(x) \quad (17)$$

$\phi_1$  and  $\phi_2$  are constant coefficients determined from the boundary conditions.

$$\phi_1 = -\phi_2 = \frac{K_1}{\lambda} \cdot \left[ \frac{(y_1+y_2)(y_1+y_2+t_{a1})}{E_1 I_1 + E_2 I_2} + \frac{1}{E_1 A_1} + \frac{1}{E_2 A_2} + (\alpha_2 - \alpha_1) \cdot \Delta T \right] - \frac{\eta \cdot q}{\lambda} \quad (18)$$

### 2.3.2 Slip distribution along the Aluminum– sandwich honeycomb interface

The following governing differential equation for the slip strain at the interface of uniformly distributed load is calculated as (Bensatallah *et al.* 2020)

$$s = (q + (\alpha_2 - \alpha_1) \cdot \Delta T) \left( \frac{\eta}{\lambda} \frac{e^{-\lambda x} - e^{\lambda x}}{e^{\frac{\lambda}{2}} + e^{-\frac{\lambda}{2}}} + \eta \cdot x \right) \quad (19)$$

$$S = \frac{(q + (\alpha_2 - \alpha_1) \cdot \Delta T) (\lambda \frac{e^{-\lambda x} - e^{\lambda x}}{e^{\frac{\lambda}{2}} + e^{-\frac{\lambda}{2}}} + x) (\frac{1}{b_2 E_1 A_1} + \frac{1}{b_2 E_2 A_2})}{\frac{(y_1+y_2)(y_1+y_2+t_{a1})}{E_1 I_1 + E_2 I_2} + \frac{1}{E_1 A_1} + \frac{1}{E_2 A_2} + (\alpha_2 - \alpha_1) \Delta T} \quad (20)$$

### 2.4 Shear stress analysis at interface 2: Aluminum beam-imperfect FGM composite

The governing differential equation for the interfacial shear stress is expressed as (Hassaine Daouadji *et al.* 2021)

$$\frac{d^2 \tau(x)}{dx^2} - \frac{b_2 \left[ \frac{(y_2+y_3)(y_2+y_3+t_{a2})}{E_2 I_2 + E_3 I_3} + \frac{1}{E_2 A_2} + \frac{1}{E_3 A_3} \right]}{\frac{t_{a2}}{G_{a2}} + \frac{t_2}{4G_2} + \frac{5t_3}{12G_3}} \tau(x) + \frac{\left[ \frac{y_2+y_3}{E_2 I_2 + E_3 I_3} \right]}{\frac{t_{a2}}{G_{a2}} + \frac{t_2}{4G_2} + \frac{5t_3}{12G_3}} V_T(x) = 0 \quad (21)$$

For simplicity, the general solutions presented below are limited to loading which is either concentrated or uniformly distributed over part or the whole span of the beam, or both. For such loading,  $d^2 V_T(x)/dx^2=0$ , and the general solution to Eq. (21) is given by

$$\tau(x) = \phi_3 \cosh(\xi x) + \phi_4 \sinh(\xi x) + \frac{(t_2+t_3)}{2\xi^2 \left( \frac{t_{a2}}{G_{a2}} + \frac{t_2}{4G_2} + \frac{5t_3}{12G_3} \right) (E_2 I_2 + E_3 I_3)} V_T(x) \quad (22)$$

Where

$$\xi = \left[ \frac{b_2 \left[ \frac{(t_2+t_3)(t_2+t_3+2t_{a2})}{4(E_2 I_2 + E_3 I_3)} + \frac{1}{E_2 A_2} + \frac{1}{E_3 A_3} + (\alpha_3 - \alpha_2) \Delta T \right]}{\frac{t_{a2}}{G_{a2}} + \frac{t_2}{4G_2} + \frac{5t_3}{12G_3}} \right]^{\frac{1}{2}} \quad (23)$$

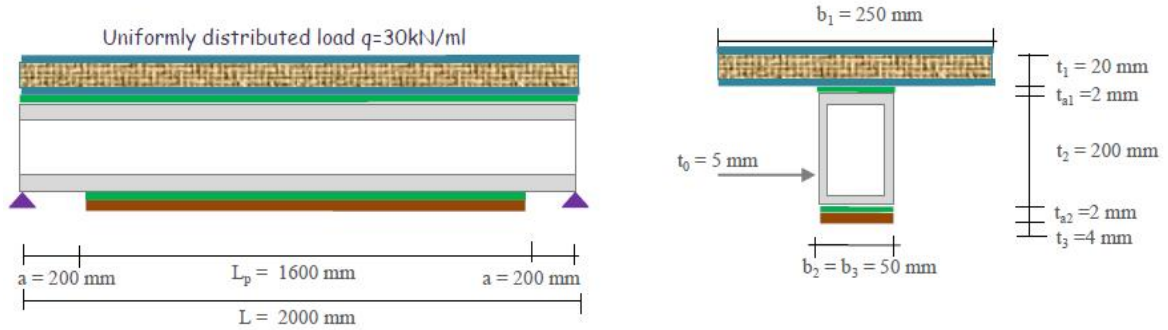


Fig. 3 Geometric characteristic of a composite aluminum- sandwich honeycomb beam strengthened by imperfect FGM plate

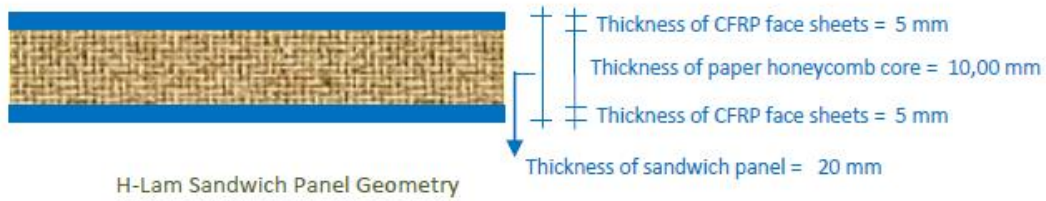


Fig. 4 Geometric characteristic of Honeycomb sandwich

In addition,  $\phi_3$  and  $\phi_4$  are constant coefficients determined from the boundary conditions. In the present study, a simply supported beam has been investigated which is subjected to a uniformly distributed load. For our case of a uniformly distributed load, the formula of the shear stress is given by the following equation

$$\tau(x) = \left[ \frac{1}{\xi} \left( \frac{t_{a2}}{G_{a2}} + \frac{t_2}{4G_2} + \frac{5t_3}{12G_3} \right) \left( \frac{y_2 M_t(0)}{E_2 I_2} - (\alpha_3 - \alpha_2) \Delta T \right) \right] e^{-\xi x} + \frac{(t_2 + t_3) \left( a \cdot q + x - \frac{e^{-\xi x}}{\xi} - q \right)}{2\xi^2 \left( \frac{t_{a2}}{G_{a2}} + \frac{t_2}{4G_2} + \frac{5t_3}{12G_3} \right) (E_2 I_2 + E_3 I_3)} \quad (24)$$

$$0 \leq x \leq L_p$$

### 3. Results: Discussion and analysis

#### 3.1 Material used

A computer code based on the preceding equations was written to compute the interfacial stresses in a composite aluminum- sandwich honeycomb beam strengthened by imperfect FGM plate under thermo-mechanical loading. The hybrid composite material was selected in the present examples as a bonded plate. However, the analysis is equally applicable to other types of composite material.

The material used for the present studies is a composite aluminum- sandwich honeycomb beam strengthened by imperfect FGM plate. The composite aluminum -sandwich honeycomb beam is subjected to a thermo-mechanical loading. A summary of the geometric and material properties is given in Table 1; Figs. 3 and 4 illustrates the dimensions of this composite wooden-concrete beam.



Table 1 Geometric and mechanical properties of the materials used

Component	Width (mm)	Depth (mm)	Young's modulus (MPa)
Adhesive layer	$b_{a1}=b_{a2}=50$	$t_{a1}=t_{a2}=2$	$E_{a1}=E_{a2}=3000$
Aluminum Beam	$b_2=50$	$t_2=200$	$E_2=65300$
CFRP for honeycomb	$b_1=250$	$t_1=70$	$E_1=140000$
GFRP for honeycomb	$b_1=250$	$t_1=70$	$E_1=50000$
KFRP for honeycomb	$b_1=250$	$t_1=70$	$E_1=106000$
Paper for honeycomb	$b_1=250$	$t_1=70$	$E_1=50$
			Ceramic: $E_3=380000$
FGM materials	$b_3=50$	$t_3=4$	FGM: $E_3$ : Variable between ceramic and metal (see equation 1 to 7)
			Metal: $E_3=70000$

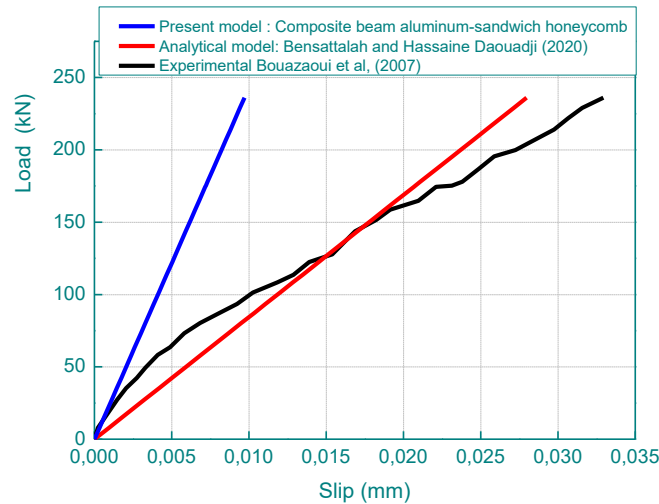


Fig. 5 Load-slip curves of composite aluminum- sandwich honeycomb beam strengthened by imperfect FGM plate: Experimental and analytical comparison of results

### 3.2 Validation of analytical model at both interfaces (Interface 1 and Interface 2)

#### 3.2.1 Interface 1

To test and validate our proposed analytical model, we compared our results of slip with those of the experimental data given by Bouazaoui *et al.* (2007) in Reims University and Bensatallah (2020), for a simply supported of a new mode of assembly of composite aluminum-sandwich honeycomb beam reinforced by imperfect FGM plate. Whose dimensions of the composite aluminum-sandwich honeycomb beam reinforced by imperfect FGM plate are shown in Figs. 3 and 4, the material properties of the composite beam are listed in Table 1. Fig. 5 shows (interface 1) the curves Load-slip of composite aluminum-sandwich honeycomb beam reinforced by imperfect FGM plate: Experimental and analytical comparison of results, the comparison of the results obtained with those of the two comparison models in the elastic domain shows a good agreement between the curves. This confirms the validation of our model. We can say that the predicted theoretical results are in reasonable agreement with the experimental results.

Table 2 Comparison of shear stress for the present method with results known in literature in Composite beam aluminum-sandwich honeycomb strengthened by imperfect FGM plate with thermo-mechanical effect

Composite beam aluminum-sandwich honeycomb strengthened by FGM porous with thermo-mechanical effect				
Theory	Composite Aluminum beam	Shear Stress		
		$q=30 \text{ kN/ml}\Delta T=0^\circ$	$q=0\Delta T=30^\circ$	$q=30 \text{ kN/ml}\Delta T=30^\circ$
	Rabahi model (2023)	11.495920		
	Benachour model (2008)	11.8138		
Present model with $\alpha=0$	Aluminum beam strengthening with perfect FGM plate (Ceramic; $k=0$ )	11.43060	4.953929	16.38454
	Aluminum beam strengthening with perfect FGM plate ( $k=5$ )	7.733758	3.513739	11.24750
	Aluminum beam strengthening with perfect FGM plate ( $k=10$ )	6.620790	3.056179	9.676972
	Aluminum beam strengthening with perfect FGM plate (Metal; $k=\infty$ )	6.519407	3.013866	9.533276
Present model with $\alpha=0,2$	Aluminum beam strengthening with imperfect FGM plate (Ceramic; $k=0$ )	11.10335	4.830804	15.93416
	Aluminum beam strengthening with imperfect FGM plate ( $k=5$ )	7.368513	3.364949	10.73347
	Aluminum beam strengthening with imperfect FGM plate ( $k=10$ )	4.876623	2.312116	7.188742
	Aluminum beam strengthening with imperfect FGM plate (Metal; $k=\infty$ )	4.056951	1.949610	6.006563

### 3.2.2 Interface 2

A comparison of the shear stresses at the interface (interface 2) of the various existing closed-form solutions and the new current solution is undertaken in this section. A Composite beam aluminum-sandwich honeycomb reinforced by imperfect FGM plate with thermo-mechanical loading is considered. A summary of the geometric and material properties is given in Table 1. The table 2 shows the comparison of shear stresses at the interface near the end of the plate for the example composite beam bonded to an imperfect FGM plate for the thermo-mechanical loading load case. Overall, the predictions of the different solutions agree closely with each other theories from the literature.

### 3.3 Parametric studies

#### 3.3.1 Effect of stiffness of sandwich honeycomb plate of the strengthened composite aluminum beam

Fig. 6 gives Distribution of interfacial slip mid along the span of composite aluminum-sandwich honeycomb beam strengthened by imperfect FGM under thermo-mechanical loading with porosity, a CFRP plate, a GFRP plate and a third in KFRP, which demonstrates the effect properties of the plate material on the sliding stresses. The results show that as the plate material becomes softer (from CFRP to KFRP to GFRP), interfacial slip decreases, as expected. Indeed, under the same load, the tensile force developed in the plate is lower, which leads to reduced interfacial slip.

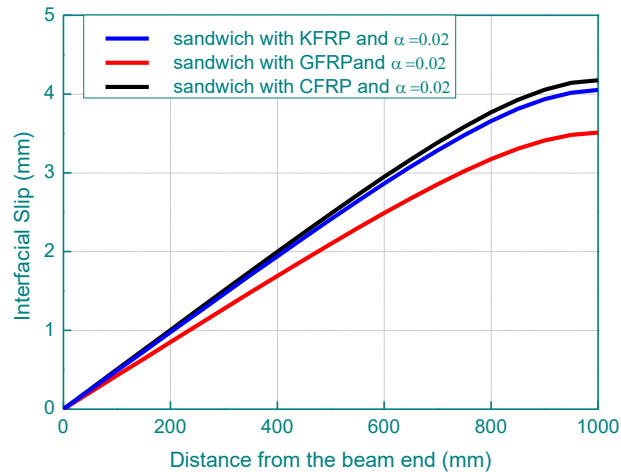


Fig. 6 Distribution of interfacial slip mid along the span of composite aluminum- sandwich honeycomb beam strengthened by imperfect FGM under thermo-mechanical loading with porosity

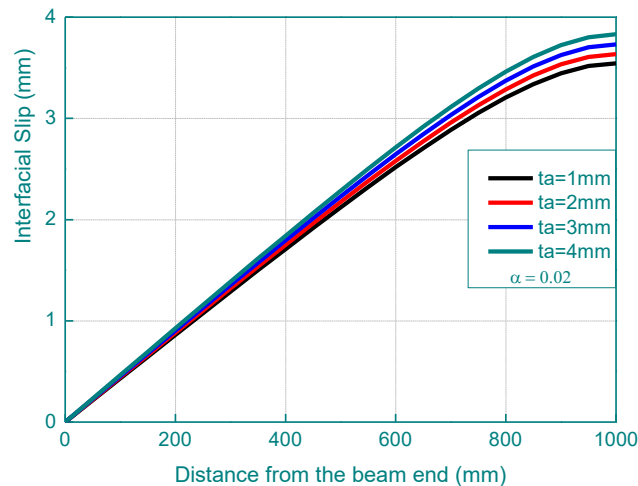


Fig. 7 Effect of adhesive thickness on the sliding of the composite aluminum- sandwich honeycomb beam strengthened by imperfect FGM under thermo-mechanical loading with porosity.

### 3.3.2 Effect of adhesive thickness of the strengthened composite aluminum beam

Shown in Fig. 7 the Effect of adhesive thickness on the sliding of the composite aluminum-sandwich honeycomb beam strengthened by imperfect FGM under thermo-mechanical loading with porosity and Table 3 the Effect of adhesive thickness on interfacial shear stress of the composite aluminum- honeycomb beam sandwich. The sliding and the shear interfacial stress is increased because of an increase in the plate thickness. This effect is similar to that of an increase in the plate elastic modulus, it can be seen from figure that the thickness of adhesive layer affects only the sliding and shear stress concentrations, hardly the stress levels. However, design of the properties and thickness of the adhesive is a difficult problem. An optimization design of the adhesive is expected.

Table 3 Effect of adhesive thickness on interfacial shear stress of the composite aluminum- sandwich honeycomb beam strengthened by imperfect FGM under thermo-mechanical

		Shear Stress (MPa)		
$t_a$ (mm)		$Q=30 \text{ KN/m}^2 \Delta T=0^\circ$	$Q=0 \text{ KN/m}^2 \Delta T=30^\circ$	$Q=30 \text{ KN/m}^2 \Delta T=30^\circ$
Porosity $\alpha=0$	1	7,5055	3,5134	11,0189
	2	6,6208	3,0562	9,6770
	3	6,0080	2,7400	8,7480
	4	5,5509	2,5046	8,0555
Porosity $\alpha=0,1$	1	6,4960	3,0776	9,5737
	2	5,7231	2,6776	8,4007
	3	5,1880	2,4010	7,5891
	4	4,7892	2,1951	6,9843
Porosity $\alpha=0,2$	1	5,5425	2,6571	8,1996
	2	4,8766	2,3121	7,1887
	3	4,4159	2,0736	6,4895
	4	4,0726	1,8961	5,9687

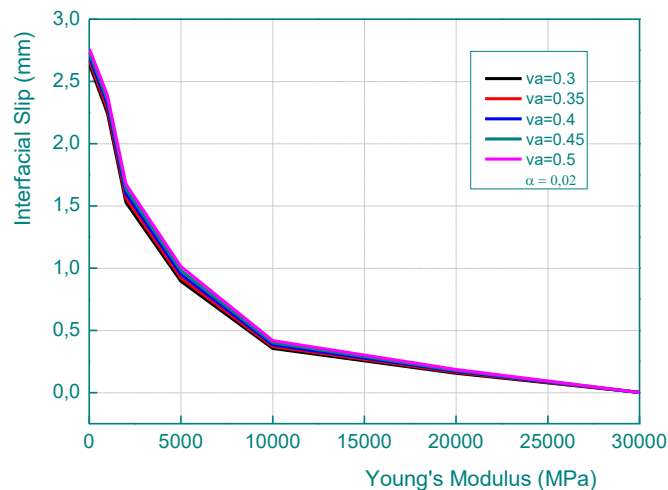


Fig. 8 Young's effect modulus of adhesive for different Poisson's ratio on the slip of the composite sandwich beam strengthened by imperfect FGM under thermo-mechanical loading with porosity

### 3.3.3 Effect of Young's modulus of the adhesive on the strengthened composite aluminum beam

The adhesive layer is a relatively soft, isotropic material and has a smaller stiffness. The six sets of Young's moduli are considered here, which are 1, 2, 3, 6, 10 and 30 GPa. The Poisson's ratio of the adhesive is also variable from the value 0.3; 0.35; 0.4; 0.45 and 0.5. As shown in Fig. 8 and Table 4, Young's effect modulus of adhesive for different Poisson's ratio on the slip and the interfacial shear stress of the composite sandwich beam strengthened by imperfect FGM under thermo-mechanical loading with porosity. The numerical results show that the property of the adhesive hardly influences the level of the sliding and interfacial shear stresses, whether shear stress, but the stress concentrations at the end of the plate increase as the Young's modulus of the adhesive increases.

Table 4 Young's effect modulus of adhesive on the interfacial shear stress of the composite aluminum-sandwich honeycomb beam strengthened by imperfect FGM under thermo-mechanical

Porosity	$E_a$ (MPa)	Shear Stress (MPa)		
		$q=30 \text{ kN/m}^2, \Delta T=0^\circ$	$q=0 \text{ kN/m}^2, \Delta T=30^\circ$	$q=30 \text{ N/m}^2, \Delta T=30^\circ$
Porosity $\alpha=0$	1000	4,92008	2,17827	7,09835
	2000	6,01332	2,74218	8,75551
	3000	6,62079	3,05618	9,67697
	6000	7,49889	3,51058	11,00947
	10000	7,97852	3,75897	11,73749
	30000	8,57659	4,06884	12,64542
Porosity $\alpha=0,1$	1000	4,23533	1,90845	6,14378
	2000	5,19153	2,40251	7,59405
	3000	5,72311	2,67761	8,40072
	6000	6,49172	3,07573	9,56745
	10000	6,91161	3,29335	10,20496
	30000	7,43525	3,56483	11,00008
Porosity $\alpha=0,2$	1000	3,59356	1,64795	5,24151
	2000	4,41807	2,07457	6,49264
	3000	4,87662	2,31212	7,18874
	6000	5,53979	2,65589	8,19568
	10000	5,90213	2,84381	8,74593
	30000	6,35404	3,07823	9,43228

Table 5 Effect of the variation of the distribution forms of porosity on the slip of the composite aluminum-sandwich honeycomb beam strengthened by imperfect FGM under thermo-mechanical

Composite beam aluminum-sandwich honeycomb strengthened by imperfect FGM with thermo-mechanical effect- $k=10$							
Distribution forms of Porosity	Porosity	Slip: $\delta(x=0)$ mm			Deflection: $\Delta(x=L/2)$ mm		
		$q=30 \text{ kN/ml}$ $\Delta T=0^\circ$	$q=0$ $\Delta T=30^\circ$	$q=30 \text{ kN/ml}$ $\Delta T=30^\circ$	$q=30 \text{ kN/ml}$ $\Delta T=0^\circ$	$q=0$ $\Delta T=30^\circ$	$q=30 \text{ kN/ml}$ $\Delta T=30^\circ$
Homogeneous Shape	$\alpha=0$	4.164	$2.505 \cdot 10^{-8}$	4.175	4.555	$2.733 \cdot 10^{-8}$	4.555
	$\alpha=0,01$	4.186	$2.516 \cdot 10^{-8}$	4.194	4.572	$2.743 \cdot 10^{-8}$	4.572
	$\alpha=0,02$	4.204	$2.530 \cdot 10^{-8}$	4.216	4.589	$2.753 \cdot 10^{-8}$	4.589
Form "V" Shape	$\alpha=0$	4.164	$2.506 \cdot 10^{-8}$	4.175	4.555	$2.733 \cdot 10^{-8}$	4.555
	$\alpha=0,01$	4.179	$2.514 \cdot 10^{-8}$	4.190	4.567	$2.740 \cdot 10^{-8}$	4.567
	$\alpha=0,02$	4.193	$2.523 \cdot 10^{-8}$	4.205	4.579	$2.748 \cdot 10^{-8}$	4.579
Form Inverted "V" Shape	$\alpha=0$	4.164	$2.505 \cdot 10^{-8}$	4.175	4.555	$2.733 \cdot 10^{-8}$	4.555
	$\alpha=0,01$	4.168	$2.507 \cdot 10^{-8}$	4.178	4.558	$2.735 \cdot 10^{-8}$	4.558
	$\alpha=0,02$	4.175	$2.512 \cdot 10^{-8}$	4.186	4.562	$2.737 \cdot 10^{-8}$	4.562
Form "X" Shape	$\alpha=0$	4.164	$2.505 \cdot 10^{-8}$	4.175	4.555	$2.733 \cdot 10^{-8}$	4.555
	$\alpha=0,01$	4.175	$2.512 \cdot 10^{-8}$	4.186	4.562	$2.737 \cdot 10^{-8}$	4.562
	$\alpha=0,02$	4.186	$2.516 \cdot 10^{-8}$	4.194	4.572	$2.743 \cdot 10^{-8}$	4.572
Form "O" Shape	$\alpha=0$	4.164	$2.505 \cdot 10^{-8}$	4.175	4.555	$2.733 \cdot 10^{-8}$	4.555
	$\alpha=0,01$	4.168	$2.507 \cdot 10^{-8}$	4.186	4.558	$2.735 \cdot 10^{-8}$	4.562
	$\alpha=0,02$	4.175	$2.512 \cdot 10^{-8}$	4.194	4.562	$2.737 \cdot 10^{-8}$	4.572

Table 6 Effect of the variation of the distribution forms of porosity on the interfacial shear stress of the composite aluminum-sandwich honeycomb beam strengthened by imperfect FGM under thermo-mechanical

Composite beam aluminum sandwich honeycomb strengthened by imperfect FGM with thermo-mechanical effect- $k=10$				
Distribution forms of Porosity	Porosity	Shear stress $\tau(x)$ MPa		
		$q=30$ kN/ml, $\Delta T=0^\circ$	$q=0$ , $\Delta T=30^\circ$	$q=30$ kN/ml, $\Delta T=30^\circ$
Homogeneous Shape	$\alpha=0$	6.620790	3.056179	9.676972
	$\alpha=0,1$	5.723107	2.677612	8.400722
	$\alpha=0,2$	4.876623	2.312116	7.188742
Form "V" Shape	$\alpha=0$	6.620790	3.056179	9.676972
	$\alpha=0,1$	6.032282	2.809007	8.841292
	$\alpha=0,2$	5.347879	2.516659	7.864540
Form Inverted "V" Shape	$\alpha=0$	6.620790	3.056179	9.676972
	$\alpha=0,1$	6.393750	2.961269	9.355022
	$\alpha=0,2$	6.359837	2.947045	9.306885
Form "X" Shape	$\alpha=0$	6.620790	3.056179	9.676972
	$\alpha=0,1$	6.426958	2.975186	9.402147
	$\alpha=0,2$	6.390036	2.959712	9.349750
Form "O" Shape	$\alpha=0$	6.620790	3.056179	9.676972
	$\alpha=0,1$	6.359837	2.947045	9.306885
	$\alpha=0,2$	8.281186	3.734361	12.01555

### 3.3.4 Effect of the variation of the distribution forms of porosity on the interfacial stresses of the Composite beam aluminum-sandwich honeycomb strengthened by FGM porous with thermo-mechanical effect

Tables 5 and 6. Show the effect of the variation of the distribution forms of porosity on the slip and interfacial shear stress of the composite aluminum-sandwich honeycomb beam strengthened by imperfect FGM under thermo-mechanical, which demonstrate the effect of material properties on shear stress. Taking into account the variation in the forms of porosity distribution and the index of this porosity. The results show that, as the material becomes softer (from the least porous material to the most porous material), the sliding and shear stress interface becomes smaller, unexpected. Same load, the reinforced resistance developed in the smaller plate, which made it possible to reduce the interfacial stresses. Interfacial shear peak plate becomes less stiff.

### 3.3.5 Effect of the variation of the degree of homogeneity of the FGM material as a function of distribution forms of porosity on the Composite beam aluminum-sandwich honeycomb strengthened by FGM porous with thermo-mechanical effect

The variation of the degree of homogeneity of the FGM material plate is an important design variable in practice. Table 7. Effect of the variation of the degree of homogeneity of the FGM material as a function of distribution forms of porosity on the interfacial shear stress of the composite aluminum-sandwich honeycomb beam strengthened by imperfect FGM under thermo-mechanical. For this problem, the rigidity of the soffit plate is of much greater significance than in the beam problem. The effects of bending deformations in the plate and axial deformations in the beam are therefore expected to become significant. It is shown that the level and concentration of interfacial stress are influenced considerably by the degree of homogeneity of the FGM material

Table 7 Effect of the variation of the degree of homogeneity of the FGM material as a function of distribution forms of porosity on the interfacial shear stress of the composite aluminum- sandwich honeycomb beam strengthened by imperfect FGM under thermo-mechanical






Composite beam aluminum sandwich honeycomb strengthened by imperfect FGM with thermo-mechanical effect					
Degree of homogeneity of FGM material	Distribution forms of Porosity				
	Homogeneous	Form "O"	Form "V"	Form Inverted "V"	Form "X"
	Shape $\alpha=0,2$	Shape $\alpha=0,2$	Shape $\alpha=0,2$	Shape $\alpha=0,2$	Shape $\alpha=0,2$
					
$k$	$\tau(x)$ MPa	$\tau(x)$ MPa	$\tau(x)$ MPa	$\tau(x)$ MPa	$\tau(x)$ MPa
0 (ceramic)	15.9340	15.9559	16.1736	16.1736	16.4008
2,5	12.9686	14.2722	12.6305	13.6481	12.6898
5	10.7334	13.5619	9.87733	11.7254	10.2688
7,5	8.64390	12.8078	8.33716	10.1951	9.44449
10	7.18869	12.0155	7.86447	9.30683	9.34970
20	6.01782	9.61409	7.90805	8.61761	9.58032
$\infty$ (metal)	6.00652	8.39951	8.33220	8.33220	10.0492

plate. The results show that, as the plate material becomes softer (from ceramic, FGM (different value of the index  $k$ ) to metal), the interfacial shear stress becomes smaller, as expected. This is because, under the same load, the tensile force developed in the plate is smaller, which leads to reduced shear stresses. We recorded a maximum value of the shear stress for form "X" of porosity distribution. Finally, we found that it is indeed a very logical statement.

#### 4. Conclusions

The Interfacial shear stress analysis of composite beam aluminum-sandwich honeycomb strengthened by imperfect FGM plate under thermo-mechanical loading (shear lag effect) were investigated by an improved theoretical method. The adherend shear deformations have been included in the theoretical analyses by assuming linear shear stress distributions through the thickness of the adherends. The classical solutions which neglect the adherend shear deformations over-estimate the non-uniformity of the adhesive stresses distributions and maximum interfacial stresses. The new solution is general in nature and may be applicable to all kinds of materials. In the final part of this paper, extensive parametric studies were undertaken by using the new solution for composite beam aluminum-sandwich honeycomb strengthened by imperfect FGM with various ratios of design parameters. Observations were made based on the numerical results concerning their possible implications to practical designs. Finally, we can conclude that, the new solution methodology is general in nature and may be applicable to the analysis of other types of composite structures.

## Acknowledgments

This research was supported by the Algerian Ministry of Higher Education and Scientific Research (MESRS) as part of the grant for the PRFU research project n° A01L02UN140120200002 and by the University of Tiaret, in Algeria.

## References

- Abderezak, R., Daouadji, T.H. and Rabia, B. (2020), “Analysis of interfacial stresses of the reinforced concrete foundation beams repairing with composite materials plate”, *Couple. Syst. Mech.*, **9**(5), 473. <http://doi.org/10.12989/csm.2020.9.5.473>.
- Abderezak, R., Daouadji, T.H. and Rabia, B. (2021), “Aluminum beam reinforced by externally bonded composite materials”, *Adv. Mater. Res.*, **10**(1), 23. <http://doi.org/10.12989/amr.2021.10.1.023>.
- Abderezak, R., Daouadji, T.H. and Rabia, B. (2021), “Fiber reinforced polymer in civil engineering: Shear lag effect on damaged RC cantilever beams bonded by prestressed plate”, *Couple. Syst. Mech.*, **10**(4), 299-316. <http://doi.org/10.12989/csm.2021.10.4.299>.
- Abderezak, R., Daouadji, T.H. and Rabia, B. (2021), “Modeling and analysis of the imperfect FGM-damaged RC hybrid beams”, *Adv. Comput. Des.*, **6**(2), 117. <http://doi.org/10.12989/acd.2021.6.2.117>.
- Abderezak, R., Daouadji, T.H. and Rabia, B. (2021), “New solution for damaged porous RC cantilever beams strengthening by composite plate”, *Adv. Mater. Res.*, **10**(3), 169. <http://doi.org/10.12989/amr.2021.10.3.169>.
- Abderezak, R., Daouadji, T.H. and Rabia, B. (2022), “Analysis and modeling of hyperstatic RC beam bonded by composite plate symmetrically loaded and supported”, *Steel Compos. Struct.*, **45**(4), 591-603. <https://doi.org/10.12989/scs.2022.45.4.591>.
- Abderezak, R., Daouadji, T.H. and Tayeb, B. (2023), “Composite aluminum-slab RC beam bonded by a prestressed hybrid carbon-glass composite material”, *Struct. Eng. Mech.*, **85**(5), 573. <https://doi.org/10.12989/sem.2023.85.5.573>.
- Abderezak, R., Rabia, B. and Daouadji, T.H. (2022), “Rehabilitation of RC structural elements: Application for continuous beams bonded by composite plate under a prestressing force”, *Adv. Mater. Res.*, **11**(2), 91-109. <https://doi.org/10.12989/amr.2022.11.2.091>.
- Addou, F.Y., Bourada, F., Meradjah, M., Bousahla, A.A., Tounsi, A., Ghazwani, M.H. and Alnujaie, A. (2023), “Impact of porosity distribution on static behavior of functionally graded plates using a simple quasi-3D HSDT”, *Comput. Concrete*, **32**(1), 87-97. <https://doi.org/10.12989/cac.2023.32.1.087>.
- Aissa, B., Rabia, B. and Tahar, H.D. (2023), “Predicting and analysis of interfacial stress distribution in RC beams strengthened with composite sheet using artificial neural network”, *Struct. Eng. Mech.*, **87**(6), 517-527. <https://doi.org/10.12989/sem.2023.87.6.517>.
- Al-Furjan, M.S.H., Habibi, M., Ghabussi, A., Safarpour, H., Safarpour, M. and Tounsi, A. (2021), “Non-polynomial framework for stress and strain response of the FG-GPLRC disk using three-dimensional refined higher-order theory”, *Eng. Struct.*, **228**, 111496. <https://doi.org/10.1016/j.engstruct.2020.111496>.
- Al-Osta, M.A., Saidi, H., Tounsi, A., Al-Dulaijan, S.U., Al-Zahrani, M.M., Sharif, A. and Tounsi, A. (2021), “Influence of porosity on the hygro-thermo-mechanical bending response of an AFG ceramic-metal plates using an integral plate model”, *Smart Struct. Syst.*, **28**(4), 499-513. <http://doi.org/10.12989/sss.2021.28.4.499>.
- Alsubaie, A.M., Alfaqih, I., Al-Osta, M.A., Tounsi, A., Chikh, A., Mudhaffar, I.M. and Tahir, S. (2023), “Porosity-dependent vibration investigation of functionally graded carbon nanotube-reinforced composite beam”, *Comput. Concrete*, **32**(1), 75-85. <https://doi.org/10.12989/cac.2023.32.1.075>.
- Belabed, Z., Tounsi, A., Al-Osta, M.A., Tounsi, A. and Minh, H.L. (2024), “On the elastic stability and free vibration responses of functionally graded porous beams resting on Winkler-Pasternak foundations via finite element computation”, *Geomech. Eng.*, **36**(2), 183-204. <https://doi.org/10.12989/gae.2024.36.2.183>.



- Benachour, A., Benyoucef, S. and Tounsi, A. (2008), "Interfacial stress analysis of steel beams reinforced with bonded prestressed FRP plate", *Eng. Struct.*, **30**(11), 3305-3315. <https://doi.org/10.1016/j.engstruct.2008.05.007>.
- Bentrar, H., Chorfi, S.M., Belalia, S.A., Tounsi, A., Ghazwani, M.H. and Alnujaie, A. (2023), "Effect of porosity distribution on free vibration of functionally graded sandwich plate using the P-version of the finite element method", *Struct. Eng. Mech.*, **88**(6), 551. <https://doi.org/10.12989/sem.2023.88.6.551>.
- Bentrar, H., Chorfi, S.M., Belalia, S.A., Tounsi, A., Ghazwani, M.H. and Alnujaie, A. (2023), "Effect of porosity distribution on free vibration of functionally graded sandwich plate using the P-version of the finite element method", *Struct. Eng. Mech.*, **88**(6), 551. <https://doi.org/10.12989/sem.2023.88.6.551>.
- Bouakaz, K., Daouadji, T.H., Meftah, S.A., Ameer, M., Tounsi, A. and Bedia, E.A. (2014), "A numerical analysis of steel beams strengthened with composite materials", *Mech. Compos. Mater.*, **50**, 491-500. <https://doi.org/10.1007/s11029-014-9435-x>.
- Bouazaoui, L., Perrenot, G., Delmas, Y. and Li, A. (2007), "Experimental study of bonded steel concrete composite structures", *J. Constr. Steel Res.*, **63**(9), 1268-1278. <http://doi.org/10.1016/j.jcsr.2006.11.002>.
- Bourada, F., Bousahla, A.A., Tounsi, A., Tounsi, A., Tahir, S.I., Al-Osta, M.A. and Do-Van, T. (2023), "An integral quasi-3D computational model for the hygro-thermal wave propagation of imperfect FGM sandwich plates", *Comput. Concrete*, **32**(1), 61-74. <https://doi.org/10.12989/cac.2023.32.1.061>.
- Bouaid, H., Rabia, B. and Daouadji, T.H. (2022), "Curvature ductility of confined HSC columns", *International Conference on Innovative Solutions in Hydropower Engineering and Civil Engineering*, Singapore, September. [https://doi.org/10.1007/978-981-99-1748-8\\_21](https://doi.org/10.1007/978-981-99-1748-8_21).
- Bouaid, H., Rabia, B. and Daouadji, T.H. (2023), "Ultimate behavior of RC beams strengthened in flexure using FRP material", *Eng. Struct.*, **289**, 116300. <https://doi.org/10.1016/j.engstruct.2023.116300>.
- Cuong-Le, T., Nguyen, K.D., Le-Minh, H., Phan-Vu, P., Nguyen-Trong, P. and Tounsi, A. (2022), "Nonlinear bending analysis of porous sigmoid FGM nanoplate via IGA and nonlocal strain gradient theory", *Adv. Nano Res.*, **12**(5), 441. <https://doi.org/10.12989/anr.2022.12.5.441>.
- Daouadji, T.H. (2013), "Analytical analysis of the interfacial stress in damaged reinforced concrete beams strengthened by bonded composite plates", *Strength Mater.*, **45**(5), 587-597. <https://doi.org/10.1007/s11223-013-9496-4>.
- Daouadji, T.H. (2017), "Analytical and numerical modeling of interfacial stresses in beams bonded with a thin plate", *Adv. Comput. Des.*, **2**(1), 57-69. <https://doi.org/10.12989/acd.2017.2.1.057>.
- Daouadji, T.H., Abderezak, R. and Rabia, B. (2022), "New technique for repairing circular steel beams by FRP plate", *Adv. Mater. Res.*, **11**(3), 171-190. <https://doi.org/10.12989/amr.2022.11.3.171>.
- Draiche, K., Bousahla, A.A., Tounsi, A., Alwabri, A.S., Tounsi, A. and Mahmoud, S.R. (2019), "Static analysis of laminated reinforced composite plates using a simple first-order shear deformation theory", *Comput. Concrete*, **24**(4), 369-378. <https://doi.org/10.12989/cac.2019.24.4.369>.
- Garg, A., Gupta, S., Chalak, H.D., Belarbi, M.O., Tounsi, A., Li, L. and Zenkour, A.M. (2023), "Free vibration analysis of power-law and sigmoidal sandwich FG plates using refined zigzag theory", *Adv. Mater. Res.*, **12**(1), 43. <https://doi.org/10.12989/amr.2023.12.1.043>.
- Hamrat, M., Bouziadi, F., Boulekbache, B., Daouadji, T.H., Chergui, S., Labed, A. and Amziane, S. (2020), "Experimental and numerical investigation on the deflection behavior of pre-cracked and repaired reinforced concrete beams with fiber-reinforced polymer", *Constr. Build. Mater.*, **249**, 118745. <http://doi.org/10.1016/j.conbuildmat.2020.118745>.
- Henni, M.A.B., Abbès, B., Daouadji, T.H., Abbès, F. and Adim, B. (2021), "Numerical modeling of hygrothermal effect on the dynamic behavior of hybrid composite plates", *Steel Compos. Struct.*, **39**(6), 751-763. <http://doi.org/10.12989/scs.2021.39.6.751>.
- Kablia, A., Benferhat, R., Daouadji, T.H. and Abderezak, R. (2023), "Free vibration of various types of FGP sandwich plates with variation in porosity distribution", *Struct. Eng. Mech.*, **85**(1), 1-14. <https://doi.org/10.12989/sem.2023.85.1.001>.
- Kaddari, M., Kaci, A., Bousahla, A.A., Tounsi, A., Bourada, F., Bedia, E.A. and Al-Osta, M.A. (2020), "A study on the structural behaviour of functionally graded porous plates on elastic foundation using a new quasi-3D model: Bending and free vibration analysis", *Comput. Concrete*, **25**(1), 37-57.

- <https://doi.org/10.12989/cac.2020.25.1.037>.
- Katiyar, V., Gupta, A. and Tounsi, A. (2022), "Microstructural/geometric imperfection sensitivity on the vibration response of geometrically discontinuous bi-directional functionally graded plates (2D FGPs) with partial supports by using FEM", *Steel Compos. Struct.*, **45**(5), 621-640. <https://doi.org/10.12989/scs.2022.45.5.621>.
- Khadimallah, M.A., Hussain, M., Khedher, K.M., Naeem, M.N. and Tounsi, A. (2020), "Backward and forward rotating of FG ring support cylindrical shells", *Steel Compos. Struct.*, **37**(2), 137-150. <http://doi.org/10.12989/scs.2020.37.2.137>.
- Khorasani, M., Lampani, L. and Tounsi, A. (2023), "A refined vibrational analysis of the FGM porous type beams resting on the silica aerogel substrate", *Steel Compos. Struct.*, **47**(5), 633. <https://doi.org/10.12989/scs.2023.47.5.633>.
- Liu, G., Wu, S., Shahsavari, D., Karami, B. and Tounsi, A. (2022), "Dynamics of imperfect inhomogeneous nanoplate with exponentially-varying properties resting on viscoelastic foundation", *Eur. J. Mech.-A/Solid.*, **95**, 104649. <https://doi.org/10.1016/j.euromechsol.2022.104649>.
- Mahmoud, S.R., Ghandourah, E.I., Algarni, A.H., Balubaid, M.A., Tounsi, A., Tounsi, A. and Bourada, F. (2023), "Stability investigation of symmetrically porous advanced composites plates via a novel hyperbolic RPT", *Steel Compos. Struct.*, **46**(4), 471. <https://doi.org/10.12989/scs.2023.46.4.471>.
- Mesbah, A., Belabed, Z., Amara, K., Tounsi, A., Bousahla, A.A. and Bourada, F. (2023), "Formulation and evaluation a finite element model for free vibration and buckling behaviours of functionally graded porous (FGP) beams", *Struct. Eng. Mech.*, **86**(3), 291-309. <https://doi.org/10.12989/sem.2023.86.3.291>.
- Rabahi, A., Adim, B., Chargui, S. and Daouadji, T.H. (2014), "Interfacial stresses in FRP-plated RC beams: effect of adherend shear deformations", *Conference on Multiphysics Modelling and Simulation for Systems Design*, Cham, December. <https://doi.org/10.1016/j.ijadhadh.2008.06.008>.
- Rabia, B., Abderezak, R., Daouadji, T.H., Abbes, B., Belkacem, A. and Abbes, F. (2018), "Analytical analysis of the interfacial shear stress in RC beams strengthened with prestressed exponentially-varying properties plate", *Adv. Mater. Res.*, **7**(1), 29. <https://doi.org/10.12989/amr.2018.7.1.029>.
- Rabia, B., Daouadji, T.H. and Abderezak, R. (2019), "Effect of distribution shape of the porosity on the interfacial stresses of the FGM beam strengthened with FRP plate", *Earthq. Struct.*, **16**(5), 601. <https://doi.org/10.12989/eas.2019.16.5.601>.
- Rabia, B., Daouadji, T.H. and Abderezak, R. (2021), "Effect of air bubbles in concrete on the mechanical behavior of RC beams strengthened in flexion by externally bonded FRP plates under uniformly distributed loading", *Compos. Mater. Eng.*, **3**(1), 41. <http://doi.org/10.12989/cme.2021.3.1.041>.
- Rabia, B., Daouadji, T.H. and Abderezak, R. (2023), "Mechanical behavior of RC beams bonded with thin porous FGM plates: Case of fiber concretes based on local materials from the mountains of the Tiaret highlands", *Couple. Syst. Mech.*, **12**(3), 241-260. <https://doi.org/10.12989/csm.2023.12.3.241>.
- Smith, S.T. and Teng, J.G. (2001), "Interfacial stresses in plated beams", *Eng. Struct.*, **23**(7), 857-871. [http://doi.org/10.1016/S0141-0296\(00\)00090-0](http://doi.org/10.1016/S0141-0296(00)00090-0).
- Tahar, H. D., Abderezak, R. and Rabia, B. (2020), "Flexural performance of wooden beams strengthened by composite plate", *Struct. Monit. Mainten.*, **7**(3), 233-259. <http://doi.org/10.12989/smm.2020.7.3.233>.
- Tahar, H.D., Boussad, A., Abderezak, R., Rabia, B., Fazilay, A. and Belkacem, A. (2019), "Flexural behaviour of steel beams reinforced by carbon fibre reinforced polymer: Experimental and numerical study", *Struct. Eng. Mech.*, **72**(4), 409-420. <https://doi.org/10.12989/sem.2019.72.4.409>.
- Tahar, H.D., Tayeb, B., Abderezak, R. and Tounsi, A. (2021), "New approach of composite wooden beam-reinforced concrete slab strengthened by external bonding of prestressed composite plate: Analysis and modeling", *Struct. Eng. Mech.*, **78**(3), 319-332. <http://doi.org/10.12989/sem.2021.78.3.31>.
- Tayeb, B. and Daouadji, T.H. (2020), "Improved analytical solution for slip and interfacial stress in composite steel-concrete beam bonded with an adhesive", *Adv. Mater. Res.*, **9**(2), 133. <http://doi.org/10.12989/amr.2020.9.2.133>.
- Tlidji, Y., Benferhat, R., Daouadji, T.H., Tounsi, A. and Trinh, L.C. (2022), "Free vibration analysis of FGP nanobeams with classical and non-classical boundary conditions using State-space approach", *Adv. Nano Res.*, **13**(5), 453. <https://doi.org/10.12989/anr.2022.13.5.453>.

- Van Vinh, P., Van Chinh, N. and Tounsi, A. (2022), "Static bending and buckling analysis of bi-directional functionally graded porous plates using an improved first-order shear deformation theory and FEM", *Eur. J. Mech.-A/Solid.*, **96**, 104743. <https://doi.org/10.1016/j.euromechsol.2022.104743>.
- Wang, Y.H., Yu, J., Liu, J.P., Zhou, B.X. and Chen, Y.F. (2020), "Experimental study on assembled monolithic steel-prestressed concrete composite beam in negative moment", *J. Constr. Steel Res.*, **167**, 105667. <https://doi.org/10.1016/j.jcsr.2019.06.004>.
- Xia, L., Wang, R., Chen, G., Asemi, K. and Tounsi, A. (2023), "The finite element method for dynamics of FG porous truncated conical panels reinforced with graphene platelets based on the 3-D elasticity", *Adv. Nano Res.*, **14**(4), 375-389. <https://doi.org/10.12989/2023.14.4.375>.
- Zine, A., Bousahla, A.A., Bourada, F., Benrahou, K.H., Tounsi, A., Bedia, E.A., ... & Tounsi, A. (2020), "Bending analysis of functionally graded porous plates via a refined shear deformation theory", *Comput. Concrete*, **26**(1), 63-74. <http://doi.org/10.12989/cac.2020.26.1.063>.
- Zohra, A., Rabia, B. and Tahar, H.D. (2023), "Critical thermal buckling analysis of porous FGP sandwich plates under various boundary conditions", *Struct. Eng. Mech.*, **87**(1), 29-46. <https://doi.org/10.12989/sem.2023.87.1.029>.